An adaptive sparse grid Navier Stokes solver in 3D based on the Finite Difference method

M. Griebel, T. Schiekofer[a]
Universität Bonn, Institut für Angewandte Mathematik
Wegelerstr. 6, D-53115 Bonn
E-mail: griebel@iam.uni-bonn.de, schiekof@iam.uni-bonn.de

Sparse grids provide an efficient representation of discrete solutions of PDEs and are mainly based on specific tensor products of 1D hierarchical basis ansatz functions. They easily allow adaptive refinement and coarsening. We present special finite differences on sparse grids which possess nearly the same properties as finite differences on full grids. Also higher order finite difference operators on sparse grids can easily be obtained. Using this approach, partial differential equations of second order can be discretized straightforwardly. These techniques are employed within a procedure for the solution of the Navier Stokes equations in 3D. Here, we apply the method of artificial compressibility and a pressure correction method.

1 Introduction to sparse grids

A detailed introduction to sparse grids can e.g. be found in [Gri97, BDZ96, BuDo97, Sch98] and the references cited therein. Yet, the most important aspects of sparse grids are presented in the following.

1.1 Hierarchical basis in 1D

The starting point for sparse grids is the piecewise hierarchical basis in 1D [Fab09, Yse86] (cf. Figure 1).

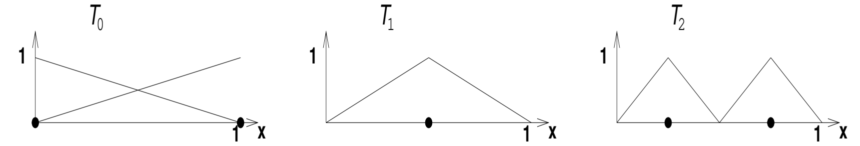

Figure 1: hierarchical basis in one dimension

First, the nodal basis $\mathcal{B}_l(\Omega) = \{\varphi_0, \ldots, \varphi_{2^l}\}$ is a set of of piecewise linear functions defined by $\varphi_i(x_j) = \delta_{ij}(x_j)$ for $i, j \in \{0, \ldots, 2^l\}$. Here, we assume $\Omega = [0,1]$ and $x_i = i \cdot 2^{-l}$. Now, the hierarchical basis $\mathcal{H}_l(\Omega)$ is defined by $\mathcal{H}_0(\Omega) \equiv \mathcal{T}_0(\Omega) \equiv \mathcal{B}_0(\Omega)$ and $\mathcal{H}_l(\Omega) = \mathcal{H}_{l-1}(\Omega) \cup \mathcal{T}_l(\Omega)$ where $\mathcal{T}_l(\Omega)$ is defined as the subset of basis functions of $\mathcal{B}_l(\Omega)$ with odd indices. Here, $\mathcal{T}_l(\Omega)$ consists of all basis function of $\mathcal{B}_l(\Omega)$ that correspond to new gridpoints, $\mathcal{T}_k(\Omega) \cap$

[a]The second author is supported by the BMBF within the project PAR-CVD, FKZ 01 IR 502 E 2

$\mathcal{T}_m(\Omega) = \emptyset$ for $k \neq m$, and the hierarchical basis $\mathcal{H}_l(\Omega)$ implies a multilevel decomposition of the space of piecewise linear functions.

1.2 Extension to several dimensions

The extension from one to two or more dimensions is straightforward using the tensor product ansatz. The quadratic scheme in the left part of Figure 2 shows a theoretically infinite tableau of supports of piecewise bilinear basis functions in two dimensions corresponding to a full grid. Each single subspace T_{i_1,i_2} contains $2^{i_1+i_2-2}$ piecewise bilinear basis functions (grid points, respectively).

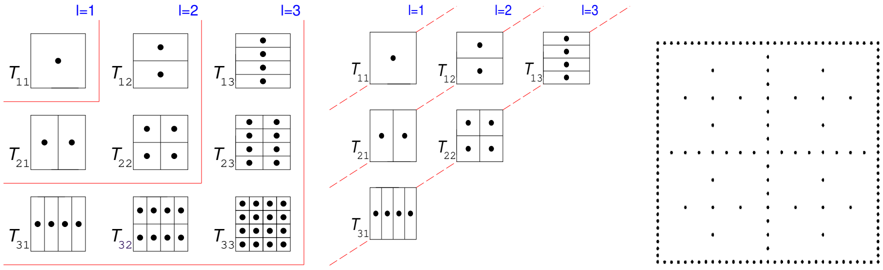

Figure 2: support of basis functions in 2 dimensions (inner subspaces), sparse grid

The volume of the support of each single basis function in the inner subspace T_{i_1,i_2} is $\mathrm{vol}(\mathrm{supp}(\varphi_{i_1,i_2})) = 2^{d-i_1-i_2}$, or generally speaking in d dimensions it is $\mathrm{vol}(\mathrm{supp}(\varphi_{i_1,\ldots,i_d})) = 2^{d-i_1-\ldots-i_d}$. Furthermore, for functions u on $\Omega_2 = [0,1]^2$, for which the mixed second derivative $\frac{\partial^4 u}{\partial x_1^2 x_2^2}$ (and also some lower mixed derivatives) are bounded on Ω_2, it has been shown ([Bun92, Zen91]) that the contribution of subspaces T_{i_1,i_2} with $i_1 + i_2 = c = \mathit{constant}$ to the interpolant of u is of the same order $\mathcal{O}(2^{-2c})$ with respect of the L_2- and the L_∞-norm and $\mathcal{O}(2^{-c})$ with respect to the to the H^1-norm. In d dimensions similar results can be shown for functions u on $\Omega_d = [0,1]^d$ if $\frac{\partial^{2d} u}{\partial x_1^2 \cdots x_d^2}$ (and also some lower mixed derivatives) are bounded on Ω_d.

On the basis of these results and considering costs versus accuracy it seems reasonable to take only a triangular scheme of subspaces T_{i_1,i_2} in the 2-dimensional case into account as indicated in the middle of Figure 2. Hence, to obtain a (regular) sparse grid one omits those subspaces in the tableau that produce much cost with only slight contributions to the interpolant. In Figure 2 a (regular) sparse grid on level 5 in two dimensions can be seen. Analogously, sparse grids in higher dimensions ($d > 2$) are obtained by omitting all subspaces $T_{i_1,\ldots,i_d}$ with $i_1 + \ldots + i_d > c = \mathit{constant}$. Adaptivity helps if functions u on Ω_d are not smooth enough or if the mixed second derivative is not bounded. Some numerical examples with this strategy are presented in section 3. A summary of properties of sparse grids as well as a comparison with properties of full grids can be found in Table 1.

Table 1: comparison of properties of sparse grids and full grids

property	regular sparse grid	full grid
accuracy in L_2	$\mathcal{O}(h^2 \cdot (\log(h^{-1})^{d-1}))$	$\mathcal{O}(h^2)$
accuracy in L_∞	$\mathcal{O}(h^2 \cdot (\log(h^{-1})^{d-1}))$	$\mathcal{O}(h^2)$
accuracy in $\|\cdot\|_A$	$\mathcal{O}(h^1)$	$\mathcal{O}(h^1)$
smoothness requirement	$\frac{\partial^{2d} u}{\partial x_1^2 \dots \partial x_d^2}$ bounded	$\frac{\partial^2 u}{\partial x_1^2}, \dots, \frac{\partial^2 u}{\partial x_d^2}$ bounded
# gridpoints	$\mathcal{O}(N \cdot (\log(N)^{d-1}))$	$\mathcal{O}(N^d)$
$d = 3, N = 2^{10}$	$1.1 \cdot 10^5$	$1.1 \cdot 10^9$
$d = 3, N = 2^{20}$	$3.3 \cdot 10^8$	$1.2 \cdot 10^{18}$

2 Finite difference operators on sparse grids

2.1 Finite difference operators

The advantage of finite differences compared to finite elements is their easy implementation in arbitrary dimensions. Finite difference operators on sparse grids for first, second or higher derivatives can all be obtained in the same way. It is well known from the full grid case that finite difference operators work on nodal values. Hence, the starting point for the sparse grid operators are also nodal values rather than hierarchical values. Now, if a discrete derivative in coordinate direction $i \in \{1, \dots, d\}$ has to be computed, one has to perform 3 steps, cf. [Sch98, Gri97]:

1. apply a transformation from the nodal basis to the hierarchical basis in each coordinate direction except i
2. apply the finite difference stencil in coordinate direction i (the stencils are just the same as in the well known full grid case) according to the local meshwidth on the respective one-dimensional gridlines
3. apply a transformation from the hierarchical basis back to the nodal basis in each coordinate direction except i

Hence, in d dimensions the sparse grid Laplace operator[b] results in

$$\mathbf{\Delta^{SG}} = \sum_{i=1}^{d} \mathbf{E_{I\setminus\{i\}}} \circ \mathbf{D_{ii}} \circ \mathbf{H_{I\setminus\{i\}}}$$

and a convective part of a partial differential equation reads

$$\vec{\beta} \cdot \nabla^{\mathbf{SG}} = \sum_{i=1}^{d} \beta_i \cdot \mathbf{E_{I\setminus\{i\}}} \circ \mathbf{D_i} \circ \mathbf{H_{I\setminus\{i\}}}.$$

[b] the superscript "SG" indicates the sparse grid operator

Here, $\mathbf{D_i}$ and $\mathbf{D_{ii}}$ denote ordinary finite difference stencils for first[c] and second derivatives whereas $\mathbf{H}_{\mathbf{I}\setminus\{\mathbf{i}\}}$ and $\mathbf{E}_{\mathbf{I}\setminus\{\mathbf{i}\}}$ denote the transformation from the nodal basis to the hierarchical basis except for coordinate direction i and vice versa ($\mathbf{I} = \{1, 2, \ldots, d\}$). The generalization to the adaptive refined case is straightforward, see [Gri97].

As in the finite element case the matrices are not sparse. But now, even for symmetric operators, we obtain non-symmetric matrices. A factorized representation allows for matrix vector multiplications in $\mathcal{O}(n)$ operations where n is the number of gridpoints. Due to the lack of symmetry we use BiCGSTAB to solve the arising linear systems of equations rather than CG. Despite the fact that we have non-symmetric matrices also for Laplace or Helmholtz problems, the eigenvalues of the matrices remain real and positive. Note that, in the case of a full grid, our approach drops down to well known finite difference stencils (cf. [Sch98]). Note that there exist first prototypes of multigrid solvers and preconditioners based on prewavelets for our finite difference discretization on sparse grids.

2.2 Consistency and stability

The finite differences on (regular) sparse grids possess the same order of consistency as comparable full grid operators. We obtain second order $\mathcal{O}(h^2)$ for the centered difference and the second derivative and first order $\mathcal{O}(h^1)$ for backward, forward and upwind differences. Here, the order of consistency in the sparse grid case is measured according to the finest occurring meshwidth. The proofs for these assertions are based on Taylor series expansions and can be found in [Sch98].

Besides, as stability and consistency lead to convergence, stability of the sparse grid finite difference operators is of major interest. The smallest eigenvalue of the two-dimensional Laplace operator on successive grids tends to $2\pi^2$ which is the smallest eigenvalue of the continuous operator. As this eigenvalue is bounded independent of h, we have stability (cf. [Hac86]). Moreover, the largest eigenvalue and the condition number increase by approximately four just as in the full grid case.

3 Numerical examples

In this section we present some numerical results using our sparse grid finite difference approach. First, two elliptic partial differential equations of second order are considered on regular as well as on adaptive sparse grids. Then, we apply our approach to the Navier Stokes equations in two and three dimensions.

[c] backward/forward difference, centered or upwind difference

3.1 Partial differential equation of second order

We first consider the Poisson equation $-\Delta u = f$ (Problem 1) in $\Omega = (0,1)^2$ with Dirichlet boundary conditions and the exact solution $u(x,y) = \sinh(\pi(1-x))\sin(\pi y)/\sinh(\pi)$. The results for different levels of discretization are given in Table 2. Here and in the following, we show the number of points involved in the sparse grid finite difference discretization and the resulting approximation error with respect to the L_2- and L_∞-norms and furthermore give their quotients on two successive levels.

Table 2: errors for Problem 1, regular sparse grid

l	P	q_P	L_∞-error	q_{L_∞}	q_1	L_2-error	q_{L_2}	q_2
2	49	-	3.15_{-3}	-	-	1.75_{-3}	-	-
3	113	2.31	7.95_{-4}	3.96	1.71	4.34_{-4}	4.03	1.74
4	257	2.27	2.00_{-4}	3.97	1.75	1.08_{-4}	4.02	1.77
5	577	2.25	5.03_{-5}	3.98	1.77	2.69_{-5}	4.01	1.78
6	1281	2.22	1.26_{-5}	4.00	1.80	6.71_{-6}	4.01	1.81
7	2817	2.20	3.15_{-6}	4.00	1.82	1.67_{-6}	4.01	1.82

In Table 2 the abbreviations l, P, q_P, q_{L_∞}, q_1, q_{L_2} and q_2 stand for level (l) and number of sparse grid points (P) and for the quotients of two successive numbers of points in a grid (q_P), errors in the L_∞-norm (q_{L_∞}), accuracy versus work involved[d] according to the L_∞-norm ($q_1 = q_{L_\infty}/q_P$), errors in the L_2-norm (q_{L_2}) and accuracy versus effort according to the L_2-norm ($q_2 = q_{L_2}/q_P$).

The quotients of the L_2- and the L_∞-error reveal second order accuracy $\mathcal{O}(h^2)$ whereas the work involved is only of order $\mathcal{O}(h^{-1}\log h)$. The quotients of accuracy versus effort approach two in the limit case in both norms whereas in the full grid case one would simply obtain a factor of one (each time you have four times more grid points the error is reduced by a factor of four). This reveals that the sparse grid approach can be interpreted as a higher order ansatz. Again, h denotes the finest occurring meshwidth.

The second problem (Problem 2) is a convection diffusion equation $-\Delta u + \vec{\beta}\nabla u + c\cdot u = f$ in $\Omega = (0,1)^2$, $\vec{\beta} = (e^{3xy}, \sin(\pi(x+y)))$, $c = 1$, with Dirichlet boundary conditions and the exact solution $u(x,y) = x^3 e^{3.5\pi y}$. The solution has a moderate boundary layer at $y = 1$. Note that, for the discretization of the ∇-term, we use the upwind difference approach here and hence only first order accuracy can be expected. In Figure 3 the exact solution of Problem 2 together with an associated adaptive sparse grid is given. The results for adaptive sparse grids are given in Table 3. Here, the quotients must be viewed in a sense of "accuracy versus work involved". As the quotients q_1 and q_2 which measure accuracy versus involved work are about one the same orders

[d] in case of a multigrid solver the work involved is proportional to the degrees of freedom

Table 3: errors for Problem 2, adaptive sparse grid

accuracy	P	q_P	L_∞-error	q_{L_∞}	q_1	L_2-error	q_{L_2}	q_2
$\varepsilon_1 = 500$	47	-	1.87_3	-	-	4.67_2	-	-
$\varepsilon_2 = \varepsilon_1/4$	106	2.26	1.84_2	10.16	4.50	7.78_1	6.00	2.65
$\varepsilon_3 = \varepsilon_2/4$	233	2.20	8.86_1	2.08	0.95	2.39_1	3.26	1.48
$\varepsilon_4 = \varepsilon_3/4$	516	2.22	3.06_1	2.90	1.31	1.73_1	1.38	0.62
$\varepsilon_5 = \varepsilon_4/4$	1135	2.20	1.38_1	2.22	1.01	6.69_0	2.59	1.18
$\varepsilon_6 = \varepsilon_5/4$	2475	2.18	6.98_0	1.98	0.91	3.33_0	2.01	0.92

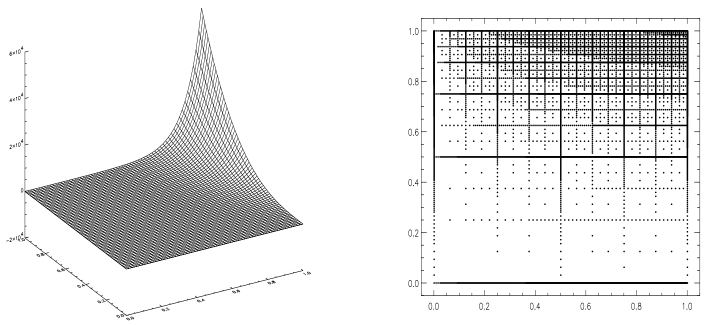

Figure 3: Exact solution of Problem 2 and an associated adaptive sparse grid

as in the regular full grid case for smooth problems are observed. For an explanation of the refinement strategy we refer to [Sch98].

3.2 Navier Stokes equations

We now want to apply our finite difference operators on sparse grids to the steady Navier Stokes equations that describe the laminar flow of incompressible and viscous fluids. Here, the equations of interest are

$$(\mathbf{u} \cdot \mathrm{grad})\mathbf{u} + \mathrm{grad}\ p = Re^{-1}\Delta\mathbf{u} + \mathbf{g} \tag{1}$$

$$\mathrm{div}\ \mathbf{u} = 0 \tag{2}$$

together with adequate boundary conditions. Here, $\mathbf{u}, p, \mathbf{g}$ and Re denote the velocities, pressure, external forces and the Reynold number, respectively. We discretize the equations using the method of the previous section. The first method we apply to solve the Navier Stokes equations is the method of artificial compressibility where we additionally take nested iteration into account. For details we refer to [PeTa90]. The second method we implemented is a pressure linked method comparable to the SIMPLE method. Here, we solve a Laplace equation with Dirichlet boundary conditions for the pressure. A detailed description of this method can be found in [Gre87].

To test the 2D version of this approach we consider the ubiquitous lid driven cavity. In Figure 4 results for the lid driven cavity problem on adaptive sparse grids for $Re = 50$ can be found. The obtained results show the expected flow of a fluid.

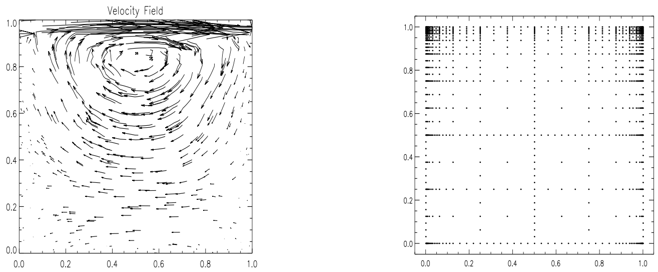

Figure 4: lid driven cavity ($Re = 50$) and adaptive sparse grid

We apply our method to a 3D test case for problems arising in simulating CVD (chemical vapor deposition) phenomena where an equation for the temperature is added to the Navier Stokes equations. In this test case fluid is

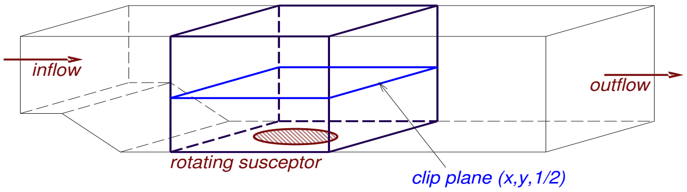

Figure 5: geometry of the reactor and domain of simulation (marked box)

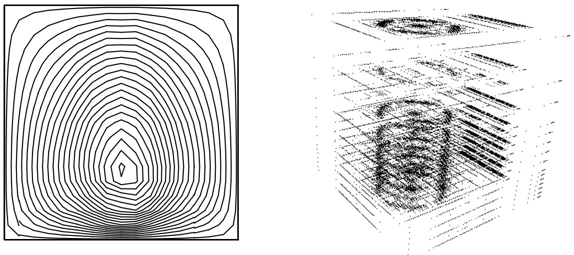

Figure 6 (CVD test case): temperature in the plane $(x, y, \frac{1}{2})$, adaptive sparse grid

flowing through a CVD reactor while the apparatus is heated from below. Here, the heat source is centered at $(\frac{1}{4}, \frac{1}{2}, 0)$ and diminishes exponentially on the boundary. Furthermore, at the bottom of the reactor, there is a rotating susceptor that has influence both on temperature and velocities. Hence, adaptive refinement is required to capture the critical criteria (e.g. jumps in the boundary conditions for the velocities) of the quantities temperature and velocities. The approximate geometry of the reactor can be seen in Figure 5. The marked box containing the susceptor (and also the heat source) is the domain of our simulations. The impact of the rotation of the susceptor on the temperature can be seen in the left of Figure 6. Here, we obtain a non-symmetric temperature distribution just as it can be observed in 'real' CVD reactors. A difference of some degrees in the temperature can be obtained in the results of simulations run by existing codes on uniform grids compared to measurements made in real life CVD reactors. Full grids hardly can resolve accurately interesting details like the rotation of a susceptor due to memory shortness. Hence, differences in simulations and measurements appear. Here, adaptive sparse grids that need only a fractional amount of the grid points of a full grid may help to overcome this difference between real life measurements in a CVD reactor and numerical simulation results.

References

[Bun92] Bungartz H.-J.: *Dünne Gitter und deren Anwendung bei der adaptiven Lösung der dreidimensionalen Poisson-Gleichung*, Ph.D. Thesis, TU München (1992)

[BDZ96] Bungartz H.-J., Dornseifer T. and Zenger C.: *Tensor product approximation spaces for the efficient numerical solution of partial differential equations*, to appear in Proc. Int. Workshop on Scientific Comput., Konya, 1996, Nova Science Publishers

[BuDo97] Bungartz H.-J. and Dornseifer T.: *Sparse grids: Recent developments for elliptic partial differential equations*, Institut für Informatik der TU München, SFB-Report 342/02/97 A, 1997.

[Cho67] Chorin A.J.: *A Numerical Method for Solving Incompressible Viscous Flow Problems*, J. of Comp. Phys., Vol. 2, pp 12–26, 1967

[Dor97] Dornseifer, T.: *Diskretisierung allgemeiner elliptischer DGL in krummlinigen Koordinatensystemen auf dünnen Gittern*, Ph.D. Thesis, TU München (1997)

[Fab09] FABER G.: *Über stetige Funktionen*, Math. Annalen, Vol. 66, pp. 81–94, 1909

[Gre87] GRESHO P.M. AND SANI R.L.: *On Pressure Boundary Conditions for the Incompressible Navier–Stokes–Equations*, International Journal for Numerical Methods in Fluids, also: Lawrence Livermore National Laboratory, Preprint UCRL-96471

[Gri91] Griebel M.: *A parallelizable and vectorizable multi-level algorithm on sparse grids in Parallel Algorithms for partial differential equations*, Notes on Numerical Fluid Mechanics, Volume 31, pp. 94-100, W. Hackbusch, ed., Vieweg, Braunschweig, 1991

[Gri97] Griebel M.: *Adaptive sparse grid multilevel methods for elliptic PDEs based on finite differences*, Notes on Numerical Fluid Mechanics, Proceedings Large Scale Scientific Computations, 7. June - 11. June, 1997, Varna, Bulgaria, Vieweg-Verlag, Braunschweig, 1998, to appear

[GrDoNe98] Griebel M., Dornseifer T. und Neunhoeffer T.: *Numerical Simulation in Fluid Dynamics – a Practical Introduction*, SIAM, Philadalphia, 1998

[Hac86] HACKBUSCH W.: *Theorie und Numerik ellipt. DGL*, Teubner, Stuttgart 1986

[PeTa90] Peyret T. and Taylor T.D.: *Computational Methods for Fluid Flow*, Springer Series in Computational Physics (corrected third printing), Stuttgart 1990

[Sch98] Schiekofer T.: *Die Methode der Finiten Differenzen auf Dünnen Gittern zur adaptiven Multilevel-Lösung partieller Differentialgleichungen*, Dissertation Universität Bonn, Institut für Angewandte Mathematik, to appear 1998

[Yse86] Yserentant H.: *On the multi-level splitting of finite element spaces*, Numer. Math., 49, pp. 379–412

[Zen91] Zenger Chr.: *Sparse Grids*, in Parallel Algorithms for PDEs; Notes on Numerical Fluid Mechanics Vol. 31, W. Hackbusch, ed., Vieweg, Braunschweig, 1991